

# On-orbit Cooperating Space Robotic Servicers Handling a Passive Object

Georgios Rekleitis and Evangelos Papadopoulos, *Senior Member, IEEE*

**Abstract**— A planning and control methodology is developed for manipulating passive objects by cooperating orbital free-flying servicers in zero gravity. Both on-off base thrusters and manipulator continuous forces are used in handling on-orbit passive objects and eliminating the effects of on-off control on them. For two different contact types, the system dynamics are presented. Using a two-layer optimization process, a planning strategy for the trajectory tracking motion of a passive object including optimal end-effector contact point selection, is developed. A model-based controller adapted to the special characteristics of the system such as the unilateral constraints and the on-off thrusting, is presented and its response is discussed, for both contact cases. The manipulation strategy is illustrated using a 3D task. For the cases studied, the system performance exhibits desirable response characteristics, such as remarkable positioning accuracy and reduced thruster fuel consumption.

**Index Terms**—Space robotics, robot cooperation, free-flying robots, object manipulation on orbit.

## I. INTRODUCTION

The growing number of orbital structures and the rapid commercialization of space require systems capable of fulfilling tasks such as construction, maintenance, astronaut assistance, docking and inspection, or even orbital debris handling and disposal. These tasks fall under the concept of On-Orbit Servicing (OOS), a relatively new but growing area of interest in space. Some of these tasks can be performed by astronauts in Extra Vehicular Activities (EVA). However, EVA is dangerous and subject to limitations such as limits to the force/torque an astronaut can apply, the motions that can be performed or even the EVA temporal constraints. To relieve astronauts from EVA, to enhance performance and to extend the range of feasible tasks, robotic servicers will be required.

As man's activities in space proliferate, passive object manipulation functions such as debris handling and deorbiting, handling of fuel-less satellites or even handling of orbital-construction parts, are going to be on demand increasingly. Large manipulators such as the Canadarm 2 (C2), mounted on a large base such as the International Space Station, are already used for object manipulation. In

such cases though, the manipulator base is so large compared to the handled object that the base can be considered quasi-fixed. Similarly, the maximum allowed payload for the space shuttle Canadarm was one third of the Shuttle's mass. To handle larger payloads, additional servicers would be required. Systems like the above are designed for limited on orbit mobility and cannot be available on demand at various locations on orbit. They also move payloads with respect to their base, and not with respect to a Cartesian frame or to another object. In the former motion, attitude disturbances may not be important, while in the later they must be considered. To address such challenges, multiple cooperating robotic servicers handling a payload of size comparable or larger than their own is proposed. To this end, the dynamics, planning and control of such systems must be studied.

Robotic OOS has been discussed a lot during the last two decades, and a number of architectures have been proposed [1]. Important robotic tasks, such as orbital assembly and debris handling, require passive object handling capabilities. The first step in the handling procedure is to securely grasp the passive object, a task called docking. Studies in this field have provided several theoretical approaches [2], [3], some of which resulted in experimental approaches [4], [5]. However, actual handling of a captured passive object has not been studied adequately and issues such as large object handling remain open. On-orbit object handling has similarities to cooperative manipulation of passive objects on Earth [6]-[17], with the additional complexities that in space no fixed ground to support the manipulators exists, thus letting momentum changes to play a key role in body motion, and that the development of control forces is of on-off nature, thus reducing system positioning capabilities.

Several prototype robotic servicers have been proposed and studied since the 1990's [4], [5], [18], [19]. Nevertheless, only a few studies exist concerning the dynamics and control of an already captured object. Dubowsky et al. proposed a control method for handling large flexible objects, aiming at reducing flexibility-induced vibrations. Robotic servicers use their thrusters as a low frequency control of rigid body motion, and their manipulators, as a high frequency control, cancelling out vibrations this motion causes on the flexible modes [20]. Fitz-Coy and Hiramatsu presented a post-docking control approach based on game theory, minimizing interaction forces, and thus helping avoid the loss of firm grasp [21]. Moosavian et al. presented a passive object manipulation method by a single servicer with multiple manipulators, aiming at an object prescribed impedance behavior, in case of contact with the environment [22]. In a simplified 2D

example, Tolia *et al.* presented a multiple servicer manipulation method of a passive object, focusing on the modularity of the system, and taking advantage of actuation and sensor redundancy, [23]. Everist *et al.* proposed a free-flying servicer concept for handling and assembling space construction rods, using proportional thrusters under PD control [24]. Orbital system thrusters, though, are of on-off control nature, leading to limit cycles in the motion of the handled object that reduce the accuracy and increase fuel consumption, compared to non on-off control. To tackle this problem, Rekleitis and Papadopoulos have proposed using a number of manipulator-equipped servicers, where both on-off thruster propulsion and manipulator continuous forces/torques are used in object handling, [25], [26], see Fig. 1. For obtaining insights, a simplified one-dimensional model for the case of firm grasping by two servicers was studied, [25]. It was shown that, since the relative motion between the servicers and the passive object only needs to be bounded, the servicers can be free to move in some envelope with respect to the passive object under scarce thruster firing, while their manipulators can apply continuous forces on the passive object, filtering the on-off thruster force effects on it and lowering fuel consumption and tracking errors [25], [26].

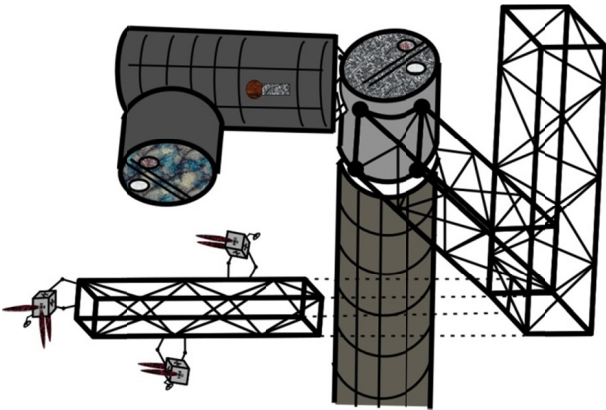


Fig. 1. Handling of a rigid passive body by a number of cooperating free-flyers equipped with manipulators, in space structure assembly operations.

The present work extends this concept and develops a strategy for handling an already captured passive object in space. The strategy uses both on-off thrusters and manipulator continuous forces/torques applied on an object by a number of robotic servicers, removing the effect of limit cycles on the object, and improving its handling both in terms of accuracy and of fuel consumed. Both the case of object firm grasp by manipulator end-effectors, and the more restrictive case of point contacts are studied in this paper. The equations of motion of the system consisting of the servicers and the object are obtained and a model-based control algorithm is developed. For both grasping modes, the controller performance is characterized by remarkable positioning accuracy with limited thruster fuel consumption, as opposed to that of pure on-off control. The robustness of the controller and the differences between the two grasp modes are also addressed.

## II. MANIPULATION BY FREE-FLYING SERVICERS

A passive object on orbit can be manipulated employing two main techniques. In the first, servicers come into direct contact with it and use their thrusters to control its motion. In the second, servicers establish contact with the object using manipulators, and control its motion with manipulator and servicer base coordinated actions.

In employing the first technique, the object motion response is essentially the same with that of a rigid free-flying system, such as a satellite, controlled by its thrusters only. At present, to protect thruster valves from the extreme space conditions, the control for these systems is on-off, initiated by a PD law acting on an error variable. However, on-off thrusting results either in chattering, which wears the thrusters and increases fuel consumption, or in deadband-induced limit cycles, that reduce fuel consumption but also positioning accuracy [27-28]. Note that although on-off thrusting is adequate in point-to-point operations, such as docking or satellite attitude corrections, it is not adequate for complex trajectory tracking as required in passive object manipulation, where position and time pairs must be achieved with small errors.

In employing the second technique, the manipulator may contact the object either with firm grasp or with point contact. In the latter case, the manipulator end-effector just touches the passive object, without being able to pull it (unilateral constraint) or to exert moments on it. Although firm grasp is safer and more practical, it is not always feasible (e.g. in active orbital debris removal), hence point contact is considered also. The use of manipulators should result in smoother passive object handling (since continuous forces are applied on it) and smaller errors, while positioning requirements for the servicer bases can be relaxed, lowering thruster firing and thus fuel consumption and thruster wear.

The aim of this paper is to study the fine positioning of a passive object in space, while eliminating on-off control effects on its motion, and minimizing the required thruster fuel. To this end, the introduction of manipulators, for both the point contact and firm grasp cases, is compared to the direct contact on-off technique. For servicers equipped with manipulators, three assumptions are made: (i) single manipulator servicers are employed for simplicity, (ii) the servicer and passive object masses and inertias are considered as much larger than those of the manipulators, while all relative accelerations and velocities are very small. For these reasons, manipulator inertia effects are neglected, (iii) gravity effects are neglected due to small maneuver durations compared to orbital times. Manipulator kinematics, i.e. manipulator posture, workspace size, and torque propagation, are taken into account.

Successful execution of a manipulation task is subject to a number of requirements, described briefly below.

- (a) Manipulator workspace constraints must be respected.
- (b) For safety reasons, thrusters pointing towards the object or towards another servicer should be turned off.
- (c1) In the *firm grasp* case, at least two servicers are needed. To control an object in six degrees of freedom (DOF), three forces and three torques must be exerted on it. Therefore, a single servicer equipped with a single

manipulator could achieve handling. Nevertheless, because of requirement (b), a single servicer will face the problem of not being able to exert thruster forces in one or more directions. Thus, even in the case of firm grasps, a number of cooperating free-flyers are needed, with two servicers being the minimum. In practice, the number of the servicers also depends on whether they are capable of applying the required magnitude of forces/ torques on the object.

(c2) In the *point contact* case, at least three single-manipulator servicers are required to produce any required force and torque vector on the passive object. This results from the fact that two manipulators with a point contact are not able to exert on the passive object a torque around an axis parallel to the line connecting the two contact points.

(d) To protect thruster valves from space conditions, continuous or pulse-width-modulation (PWM) thruster control is avoided in space. This is because the generation of low control thrusts (e.g when the tracking errors are small), requires rapid thruster switching (up to several thousand times per second). However, electromechanical thruster valves cannot follow rapid PWM commands, deteriorating controller response and performance. Rapid switching may result in valve closing before it has fully opened, or opening before it has fully closed, resulting in nozzle ice formation, deterioration of thruster performance, and eventual damages. For example, the performance of thrusters deteriorates to levels below 80%, if the duration of thrust pulses is less than 300 ms, even for 1N thrusters [29]. Simple on-off or Pulse Width Frequency (PWPF) modulation, both with minimum on/off times, are not subject to these limitations and are preferred in space [30-33]. However, even these are used in satellite attitude control where thruster firing is sparse, and not in trajectory tracking, where the controller must update thrust values several times per second.

(e) In the *point contact* case, manipulators can only push a passive body, introducing unilateral constraints and complicating manipulation. Such issues have been studied for terrestrial systems, but not for systems in zero-g, where the absence of a fixed base or of gravity pulling all bodies towards the same direction, makes the aspect of losing contact a critically important parameter. Thus, to avoid end-effector slipping, or risking losing the object, the applied forces must stay within the local friction cone.

Since the focus of this work is on minimizing thruster fuel during accurate object cooperative manipulation on orbit, and having introduced the manipulation concepts as well as the related assumptions and requirements, an important question arises: Is the introduction of manipulators beneficial for passive object manipulation? Or more specifically, can they result in accurate trajectory tracking control of a passive object not subject to limit cycles, while limiting thruster fuel use? Next, we will demonstrate that the answer is affirmative on both counts.

### III. SPATIAL SYSTEM DYNAMICS

The dynamics of a system of  $n$  orbital robotic servicers controlling a rigid passive body via manipulators is studied next. The equations of motion for passive object ( $i=0$ ) and free-flying servicer bases ( $i=1, \dots, n$ ) have the form [34]:

$$\mathbf{H}_i \ddot{\mathbf{q}}_i + \mathbf{C}_i(\mathbf{q}_i, \dot{\mathbf{q}}_i) = \mathbf{Q}_i \quad (1)$$

where  $\mathbf{q}_i$  are the generalized coordinates for the object ( $i=0$ ) and the servicer bases ( $i=1, \dots, n$ ),

$$\mathbf{q}_i^T = [\mathbf{r}_i^T, \boldsymbol{\theta}_i^T]^T = [x_i, y_i, z_i, \theta_i, \varphi_i, \psi_i]^T \quad (2)$$

where  $[x_i \ y_i \ z_i]^T$  is the position vector  $\mathbf{r}_i$  of body  $i$  with respect to the Cartesian frame and  $[\theta_i \ \varphi_i \ \psi_i]^T$  denote the Euler angles  $\boldsymbol{\theta}_i$  of the same body. If the attitude is close to an Euler angle singularity, the attitude description is switched to a different Euler angle set. Because of assumption (ii), the manipulators act as end-effector force/torque transmission to the servicer base.  $\mathbf{H}_i$  are the  $6 \times 6$  mass matrices of body  $i$ :

$$\begin{aligned} \mathbf{H}_i &= \begin{bmatrix} \text{diag}(m_i, m_i, m_i) & \mathbf{0}_{3 \times 3} \\ \mathbf{0}_{3 \times 3} & \mathbf{E}_i^T \mathbf{R}_i \mathbf{I}_i \mathbf{R}_i^T \mathbf{E}_i \end{bmatrix} = \\ &= \begin{bmatrix} \mathbf{I}_{3 \times 3} & \mathbf{0}_{3 \times 3} \\ \mathbf{0}_{3 \times 3} & \mathbf{E}_i^T \end{bmatrix} \begin{bmatrix} \text{diag}(m_i, m_i, m_i) & \mathbf{0}_{3 \times 3} \\ \mathbf{0}_{3 \times 3} & \mathbf{R}_i \mathbf{I}_i \mathbf{R}_i^T \mathbf{E}_i \end{bmatrix} = \mathbf{E}_i^* \mathbf{H}_i^* \end{aligned} \quad (3)$$

where  $\mathbf{I}_{3 \times 3}$  is the  $3 \times 3$  identity matrix,  $\mathbf{R}_i$  is the rotation matrix transforming vectors from the frame  $i$  to the Cartesian frame,  $\mathbf{I}_i$  and  $m_i$  are the inertia matrix and mass of body  $i$  respectively,  $\mathbf{E}_i$  is a  $3 \times 3$  matrix mapping the Euler rates  $\dot{\boldsymbol{\theta}}_i$  of body  $i$  to its angular velocity  $\boldsymbol{\omega}_i$ :

$$\boldsymbol{\omega}_i = \mathbf{E}_i \dot{\boldsymbol{\theta}}_i \quad (4)$$

$\mathbf{C}_i$  are  $6 \times 1$  vectors containing the nonlinear velocity terms,

$$\begin{aligned} \mathbf{C}_i &= \begin{bmatrix} \mathbf{0}_{1 \times 3} \\ \left( \mathbf{E}_i^T (\mathbf{R}_i \mathbf{I}_i \mathbf{R}_i^T \dot{\mathbf{E}}_i \dot{\boldsymbol{\theta}}_i + \mathbf{E}_i \dot{\boldsymbol{\theta}}_i \times \mathbf{R}_i \mathbf{I}_i \mathbf{R}_i^T \mathbf{E}_i \dot{\boldsymbol{\theta}}_i) \right)^T \end{bmatrix}^T = \\ &= \mathbf{E}_i^* \begin{bmatrix} \mathbf{0}_{1 \times 3} \\ \mathbf{C}_i^{*T} \end{bmatrix}^T \end{aligned} \quad (5)$$

and  $\mathbf{Q}_i$  ( $i=1, \dots, n$ ) are  $6 \times 1$  vectors that include thruster forces, reaction wheel moments and manipulator forces/ torques acting on the  $i^{\text{th}}$  servicer base,

$$\mathbf{Q}_i = \begin{bmatrix} \sum_{j=1}^{n_i} \mathbf{f}_{ij} + \mathbf{f}_{bi} \\ \mathbf{E}_i^T \left( \mathbf{n}_i + \mathbf{n}_{bi} + \sum_{j=1}^{n_i} (\mathbf{d}_{ij} \times \mathbf{f}_{ij}) + \mathbf{p}_i \times \mathbf{f}_{bi} \right) \end{bmatrix}, \quad \begin{matrix} i=1, \dots, n \\ j=1, \dots, n_i \end{matrix} \quad (6)$$

where  $n_i$  is the number of thrusters,  $\mathbf{f}_{ij}$  and  $\mathbf{n}_i$  are the thruster forces and reaction wheel moments acting on the  $i^{\text{th}}$  servicer base,  $\mathbf{f}_{bi}$  and  $\mathbf{n}_{bi}$  are the forces and moments transmitted to the  $i^{\text{th}}$  servicer base by its manipulator,  $\mathbf{d}_{ij}$  is the vector locating the  $j^{\text{th}}$  thruster of the  $i^{\text{th}}$  servicer base with respect to the base CM, and  $\mathbf{p}_i$  is the position vector locating the  $i^{\text{th}}$  manipulator mount with respect to the base CM, (see Fig. 2).

The manipulators can be attached to the object through a firm grasp or through a contact point. In the case of *firm grasp*, the vector  $\mathbf{Q}_0$  includes forces and moments applied on the passive object by the  $n$  end-effectors:

$$\mathbf{Q}_0 = \begin{bmatrix} \mathbf{q}_{f0} \\ \mathbf{q}_{n0} \end{bmatrix} = \begin{bmatrix} \sum_{i=1}^n \mathbf{f}_{Ei} \\ \mathbf{E}_i^T \left( \sum_{i=1}^n (\mathbf{d}_i \times \mathbf{f}_{Ei}) + \mathbf{n}_{Ei} \right) \end{bmatrix} \quad (7)$$

where  $\mathbf{f}_{Ei}$ ,  $\mathbf{n}_{Ei}$  are respectively the forces and moments applied to the passive object by the  $i^{\text{th}}$  end-effector, and  $\mathbf{d}_i$  is

the vector locating the  $i^{\text{th}}$  manipulator contact point  $\mathbf{A}_i$  at the passive object, with respect to its CM, see Fig. 2.

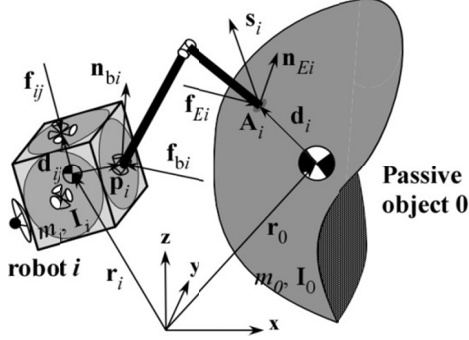


Fig. 2. Passive object (0) and the  $i^{\text{th}}$  free-flyer with a single manipulator.

In the case of *point contact*, (1)-(6) still hold; however here, end-effectors cannot apply torques. Thus (7) becomes

$$\mathbf{Q}_0 = \begin{bmatrix} \mathbf{q}_{f0} \\ \mathbf{q}_{n0} \end{bmatrix} = \begin{bmatrix} \sum_{i=1}^n \mathbf{f}_{Ei} \\ \mathbf{E}_i^T \sum_{i=1}^n (\mathbf{d}_i \times \mathbf{f}_{Ei}) \end{bmatrix} \quad (8)$$

Combining the above equations for all the  $n + 1$  bodies to a single matrix equation, the following is obtained:

$$\mathbf{H}\ddot{\mathbf{q}} + \mathbf{C}(\mathbf{q}, \dot{\mathbf{q}}) = \mathbf{Q} \quad (9)$$

where:

$$\mathbf{q} = [\mathbf{q}_0^T, \mathbf{q}_1^T, \mathbf{q}_2^T, \dots, \mathbf{q}_n^T]^T \quad (10)$$

$$\mathbf{H} = \text{diag}[\mathbf{H}_0, \mathbf{H}_1, \mathbf{H}_2, \dots, \mathbf{H}_n] \quad (11)$$

$$\mathbf{C} = [\mathbf{C}_0^T, \mathbf{C}_1^T, \mathbf{C}_2^T, \dots, \mathbf{C}_n^T]^T \quad (12)$$

$$\mathbf{Q} = [\mathbf{Q}_0^T, \mathbf{Q}_1^T, \mathbf{Q}_2^T, \dots, \mathbf{Q}_n^T]^T \quad (13)$$

In the *point contact* case, and in accordance to (c2), three servicers are needed, as opposed to at least two for the *firm grasp* case, see (c1). In the rest of the paper, for comparison reasons, we assume three servicers for both cases.

#### IV. CONTROL DESIGN AND STABILITY

In deriving a controller to eliminate errors, a number of methodologies can be used. Nevertheless, systems such as the one in discussion are highly nonlinear; in such cases, backstepping [35] can accommodate nonlinearities directly and is opted here. According to this method, we “step back” at each iteration, in order to create the control inputs from the simple subsystems of a more complex dynamic model. By transforming into new variables at each iteration, a nonlinear system can be led to display linear behavior, if there are no uncertainties on the dynamic system modeling. Since backstepping can avoid the elimination of nonlinear quantities in the controller, important for stability and trajectory tracking, it ensures the controlled system stability.

In the *firm grasp* case, the backstepping methodology results in a model-based controller, which is used to compute the necessary inertial forces and moments to be applied to the passive object, as follows,

$$\mathbf{Q}_0 = [\mathbf{0}_{1 \times 3}, \mathbf{C}_0^{*T}]^T + \mathbf{H}_0 (\ddot{\mathbf{q}}_{0,d} + \mathbf{K}_{P0} \mathbf{e}_0 + \mathbf{K}_{D0} \dot{\mathbf{e}}_0) \quad (14)$$

where  $\mathbf{e}_0 = \mathbf{q}_{0,d} - \mathbf{q}_0$ ,  $\mathbf{q}_{0,d}$  is the passive object desired trajectory, and  $\mathbf{K}_{P0}$ ,  $\mathbf{K}_{D0}$  are constant gain matrices.

Note that model-based control such as the one in (14) uses knowledge of inertial properties, which may not be available always, as is the case with non man-made objects. In those cases, these properties can be obtained by parameter identification methods, such as those in [36]-[38].

The  $\mathbf{Q}_0$  forces and moments in (14) must be applied by the three end-effectors grasping the passive object, i.e. by the three  $\mathbf{f}_{Ei}$  forces and three  $\mathbf{n}_{Ei}$  moments. However, these are subject to constraints. As mentioned earlier, thrusters facing the passive object are deactivated. Therefore, no forces are available to push a servicer away from the passive object, if its distance is less than a preset threshold. This task can be accomplished by its manipulator through the application of an appropriate reaction  $\mathbf{f}_{bi}$ , see (6). The free-flying servicer controller (presented later on) calculates the required repulsive force  $\mathbf{f}_{ij,r}$  to push the servicer away from the object. This force though, is applied as a component of the manipulator reaction  $\mathbf{f}_{bi}$ . Thus, to move the servicer away from the object, this component of  $\mathbf{f}_{bi}$ , must be at least equal to the calculated  $\mathbf{f}_{ij,r}$ . Contact force  $-\mathbf{f}_{Ei}$  is subject to the same constraint, since, due to assumption (ii),  $\mathbf{f}_{bi}$  is equal to  $-\mathbf{f}_{Ei}$ . Thus, if there is need for a repulsive force for the  $i^{\text{th}}$  servicer along the  $r$ -direction in the no-thrusting area, (15) must hold:

$$(\mathbf{f}_{bi} \cdot \hat{\mathbf{r}}) \hat{\mathbf{r}} = -(\mathbf{f}_{Ei} \cdot \hat{\mathbf{r}}) \hat{\mathbf{r}} \geq \mathbf{f}_{ij,r}, \quad i = 1, 2, 3 \quad (15)$$

where  $\hat{\mathbf{r}}$  denotes the unit vector along the  $r$ -direction.

Equations (7), (14) and (15) must hold for the end-effector forces  $\mathbf{f}_{Ei}$  and moments  $\mathbf{n}_{Ei}$ . Although (14) dictates the generalized forces  $\mathbf{Q}_0$  to act on the object,  $\mathbf{f}_{Ei}$  and  $\mathbf{n}_{Ei}$  cannot be calculated by equating (7) and (14) due to redundancy and the existence of constraints. Therefore, a method for resolving applied to end-effectors forces must be employed.

Several methods for force distribution, developed for terrestrial fixed-base systems, exist in the literature, for example [39] – [43], depending on the problem solved, i.e. number of contacts, type of contacts, type of motion expected, etc. On orbit, no fixed bases exist, as servicer bases are “flying” consuming scarce thruster fuel. To address the on orbit problem, a two-layered optimization method is introduced. The first layer aims at lowering the demands in control forces/ moments and subsequently in thruster fuel. This is because on orbit, the applied control forces/ moments on the passive object appear as disturbances on the servicers, and their rejection requires use of reaction wheels and thrusters. This layer mainly is used to obtain a force distribution; it is not critical for this distribution to be the optimal one. The second layer is developed so that the maximum control forces/moments needed are further reduced by identifying the optimal set of contact points, thus further lowering the fuel consumption. Having set up the problem as described, we adopt an appropriate constrained nonlinear optimization routine to yield both end-effector forces/moments and contact point locations.

Note that the two-layer optimization yielding the optimal contact points does not need to be executed in real time. In fact, it must be performed off-line, so as to obtain the optimal contact points, subject to geometric constraints, as preparation for the actual motion. During the actual motion, only the first-layer of the optimization method needs to be running, to resolve the required control force/ moments to the end-effectors, while the contact points are assumed to be given. This improves the execution time of the algorithm.

*First layer.* We set the three end-effector forces  $\mathbf{f}_{Ei}$  and the three end-effector moments  $\mathbf{n}_{Ei}$ , as the design parameters. Equation (7) is a linear constraint, while (15) is a non-linear constraint to be observed. Applying (14), the desired trajectory provides the required generalized object forces. Then, the optimization process returns the contact forces  $\mathbf{f}_{Ei}$  and moments  $\mathbf{n}_{Ei}$  that must be applied by the manipulators so that the object trajectory is followed, the forces/moments norm is minimized and the constraints observed. To that end, the performance index is chosen as,

$$\Lambda_1(t) = \frac{1}{2} \min_{\mathbf{n}_{Ei}, \mathbf{f}_{Ei}} \left( \sum_{i=1}^3 (\mathbf{f}_{Ei}^2) + w_2 \sum_{i=1}^3 (\mathbf{n}_{Ei}^2) \right) \quad (16)$$

so that the weighted sums of the squared norms of both the applied forces and moments is minimized. In (16),  $w_2$  is a weighting factor with appropriate units. The initial guess for each optimization step is the  $\mathbf{f}_{Ei}$  and  $\mathbf{n}_{Ei}$  of the previous step, while for the first step, the initial guess is  $\mathbf{f}_{Ei} = \mathbf{n}_{Ei} = \mathbf{0}$ .

The case of *point contacts* is described by (1) to (12), where (7) is replaced by (8). The model-based controller of (14) is used again. In this case, though, unilateral constraints are introduced for the contact forces  $\mathbf{f}_{Ei}$ . To avoid loss of contact, these forces must have a normal component towards the object. Thus the following constraint must hold

$$-\mathbf{f}_{Ei} \cdot \mathbf{s}_i < 0, \quad i = 1, 2, 3 \quad (17)$$

where  $\mathbf{s}_i$  is the unit vector at the  $i^{\text{th}}$  contact point  $\mathbf{A}_i$ , perpendicular to the surface of the passive object and facing outwards. In addition, these forces must remain within the friction cone of the contacting surfaces, so that slip of the end-effector on the surface of the passive object is avoided. Therefore, an additional constraint for  $\mathbf{f}_{Ei}$  must hold,

$$\text{atan2}(\|\mathbf{s}_i \times (-\mathbf{f}_{Ei})\|, -\mathbf{f}_{Ei} \cdot \mathbf{s}_i) \leq \text{atan}(\mu_i), \quad i = 1, 2, 3 \quad (18)$$

where  $\mu_i$  is the corresponding friction coefficient between the two contacting surfaces. In (18), function  $\text{atan2}$  is used to take into account the direction of  $\mathbf{f}_{Ei}$ .

Thus, in this case, (17) and (18) apply as additional linear and non-linear constraints respectively and (8) is used as a linear constraint, while (14) is again used as a non-linear constraint. Moreover, the return of the optimization process includes only the forces  $\mathbf{f}_{Ei}$ , applied on the passive object by the servicer manipulators. Thus, the performance index in (16) is reduced to,

$$\Lambda_1(t) = \frac{1}{2} \min_{\mathbf{f}_{Ei}} \sum_{i=1}^3 (\mathbf{f}_{Ei}^2) \quad (19)$$

thus minimizing the sum of the squared applied forces.

The required generalized forces  $\mathbf{Q}_0$  are resolved into the nine contact force components  $\mathbf{f}_E$  by optimization. The two vectors are related by:  $\mathbf{A} \mathbf{f}_E = \mathbf{Q}_0$ , where the  $6 \times 9$  matrix  $\mathbf{A}$

depends on the positions of the three contact points, with respect to the passive object center of mass. Solution to this problem requires that the matrix  $\mathbf{A} \mathbf{A}^T$  is of full rank, i.e six. This holds true always if at least two of the contact points do not coincide with the passive object center of mass. Under this assumption, the problem of force distribution has infinite solutions, as stated in requirement c2. As is true for all optimization techniques, a local minimum may result, pointing to a suboptimal solution. However, the primary task for the optimization, is to resolve the  $\mathbf{Q}_0$  to the three contact forces; this task is achieved still.

*Second Layer.* Since the fuel consumption depends on the locations of the contact points, it is beneficial to search for optimal contact point locations. To this end, an additional optimization is set up, having the coordinates of the contact point vectors  $\mathbf{d}_i$  as the design parameters. This search can be done offline, i.e. before the actual trajectories are executed. The performance index is now of min-max type,

$$\Lambda_2 = \min_{\mathbf{d}_i} \left( \max_t \Lambda_1(t) \right) \quad (20)$$

where the maximization over time  $t$  means that, for a given set of  $\mathbf{d}_i$ , the trajectory tracking motion is simulated and the overall  $\max \Lambda_1(t)$ , i.e. the worse force requirement over time is obtained. The optimization process then chooses a different set of  $\mathbf{d}_i$  until  $\max \Lambda_1(t)$  is minimized during object desired motion. The procedure yields the optimal contact point vectors  $\mathbf{d}_i$ , subject to geometrical constraints defined by the object geometry. With the completion of the optimization process, the optimal contact points for the free-flying servicers are obtained.

Next, the design of the servicer controllers, both in terms of manipulator and in terms of servicer base position and attitude (pose), is presented. Planning the desired servicer trajectory is a complex process, as the servicer manipulator will have to apply the required  $\mathbf{f}_{Ei}$  on the object while maintaining a desired pose of its base that takes into account workspace and collision avoidance requirements. To this end, appropriate initial servicer base pose with respect to the passive object is chosen. It is then desired that it is maintained within certain safety limits, throughout the motion. Hence, the desired servicer base trajectory  $\mathbf{q}_{i,d}$  is computed based on the object trajectory and sent to its motion controller, presented next.

In the case of *firm grasp*, the servicer motion controller takes as feedback the pose of the servicer base and uses it to compute the motion tracking errors, with respect to  $\mathbf{q}_{i,d}$ . Employing a model-based controller, the control inputs on a servicer are given by,

$$\left[ \sum_{j=1}^6 (\mathbf{f}_{ij}^T), \mathbf{n}_i^T \right]^T = \mathbf{H}_i^* (\ddot{\mathbf{q}}_{i,d} + \mathbf{K}_{Pi} \mathbf{e}_i + \mathbf{K}_{Di} \dot{\mathbf{e}}_i) + \mathbf{W}_i \quad (21)$$

where,

$$\mathbf{W}_i = \left[ -\mathbf{f}_{bi}^T, \left( \mathbf{C}_i^* - \mathbf{n}_{bi} - \sum_{j=1}^6 (\mathbf{f}_{ij} \times \mathbf{d}_{ij}) + \mathbf{f}_{bi} \times \mathbf{p}_i \right)^T \right]^T \quad (22)$$

The  $\mathbf{K}_{Pi}$ ,  $\mathbf{K}_{Di}$  are control gain diagonal matrices,  $\mathbf{H}_i^*$  and  $\mathbf{C}_i^*$  are defined in (3) and (5),  $\mathbf{e}_i = \mathbf{q}_{i,d} - \mathbf{q}_i$  is the tracking

error, and  $\mathbf{f}_{bi}$ ,  $\mathbf{n}_{bi}$  are the reaction forces and moments transmitted to the  $i^{\text{th}}$  servicer base by its manipulator.

To apply the controller given by (21) and (22), the reaction force  $\mathbf{f}_{bi}$  and moment  $\mathbf{n}_{bi}$  must be available. These are related to the manipulator end-effector force  $\mathbf{f}_{Ei}$  and torque  $\mathbf{n}_{Ei}$  by the manipulator force transmission equation,

$$\begin{bmatrix} \mathbf{J}_i \\ \mathbf{0}_{3 \times 3} & \mathbf{I}_{3 \times 3} \end{bmatrix}^T \begin{bmatrix} \mathbf{f}_{Ei} \\ \mathbf{n}_{Ei} \end{bmatrix} = \begin{bmatrix} \mathbf{f}_{bi} \\ \mathbf{n}_{bi} \end{bmatrix} \quad (23)$$

where  $\mathbf{J}_i$  is a  $3 \times 6$  matrix, function of manipulator posture, which resolves the end-effector force  $\mathbf{f}_{Ei}$  and torque  $\mathbf{n}_{Ei}$  to the base. Because of assumption (ii), (23) yields  $\mathbf{f}_{bi} = -\mathbf{f}_{Ei}$ . Resolving  $\mathbf{f}_{Ei}$  and  $\mathbf{n}_{Ei}$  to joint torques is achieved using the manipulator end-effector Jacobian, omitted here for brevity. Taking into account the very slow motions of space systems and their design specifications, it is reasonable to assume that manipulator actuators will be able to provide the required joint torques.

Equation (21) can be separated into two parts. The upper part, consisting of the first three equations, is independent of  $\mathbf{n}_i$  and thus can be solved for the thruster forces  $\mathbf{f}_{ij}$ , with  $\mathbf{f}_{bi}$  given by (23). Since the thrusters are on-off, the continuous  $\Sigma \mathbf{f}_{ij}$  must be approximated using a switching strategy. This strategy includes the following steps: (a) transformation of the  $\Sigma \mathbf{f}_{ij}$  to the corresponding servicer base frame (b) projection of the force along the three thruster axes, obtaining three bi-lateral continuous forces, (c) turning each thruster on, when the corresponding continuous force value exceeds a preset threshold value  $f_t$ . The result of this strategy is six uni-lateral on-off  $\mathbf{f}_{ij}$  forces. This controller will result in adequate bounded errors, such as the ones achieved in satellite attitude control. The on-off  $\mathbf{f}_{ij}$  can be used in the lower part of (21) along with  $\mathbf{f}_{bi}$  and  $\mathbf{n}_{bi}$ , in order to obtain  $\mathbf{n}_i$ .

Since wheel-applied moments are subject to limits, moments exceeding these limits can be applied by employing pairs of on-off thrusters. In this case, continuous  $\mathbf{n}_i$  of (21), (22) is also discretized, using the same switching strategy as in the case of  $\mathbf{f}_{ij}$ , with a preset threshold value  $n_t$ .

Recall at this point that the computation of the  $\mathbf{f}_{ij,r}$  required to keep the servicer away from the passive object, and needed in (15), is yet to be defined. This force is obtained by employing model-based control. To this end, a control force  $\mathbf{F}_{mb,i}$  is calculated first according to,

$$\mathbf{F}_{mb,i} = \text{diag}(m_i, m_i, m_i) \left( \ddot{\mathbf{r}}_{i,d} + \mathbf{K}_{rPi} \mathbf{e}_{r_i} + \mathbf{K}_{rDi} \dot{\mathbf{e}}_{r_i} \right) \quad (24)$$

where  $\mathbf{K}_{rPi}$  and  $\mathbf{K}_{rDi}$  are control gain diagonal matrices, while  $\mathbf{e}_{r_i} = \mathbf{r}_{i,d} - \mathbf{r}_i$  is the error between the desired position of the servicer  $\mathbf{r}_{i,d}$  and the actual position  $\mathbf{r}_i$  defined in (2). When the direction of  $\mathbf{s}_i$ , defined in (17), lays in the no-thrusting area, and depending on the sign of  $\mathbf{F}_{mb,i}$ 's component along the direction of  $\mathbf{s}_i$ , the need for the repulsive force  $\mathbf{f}_{ij,r}$  is decided. A negative sign for this component implies the need for a repulsive force, to push the servicer away from the object, and equal to the component of the  $\mathbf{F}_{mb,i}$  along the direction of  $\mathbf{s}_i$ . A positive sign implies the opposite. In this case, the force can be supplied by the thrusters, and thus,  $\mathbf{f}_{ij,r}$  is zero. Therefore,  $\mathbf{f}_{ij,r}$  is obtained as:

$$\mathbf{f}_{ij,r} = \begin{cases} (\mathbf{F}_{mb,i} \cdot \mathbf{s}_i) \mathbf{s}_i & \text{if } \text{sgn}((\mathbf{F}_{mb,i} \cdot \mathbf{s}_i) \mathbf{s}_i) < 0 \\ 0 & \text{if } \text{sgn}((\mathbf{F}_{mb,i} \cdot \mathbf{s}_i) \mathbf{s}_i) \geq 0 \end{cases} \quad (25)$$

Note that controllers (24) and (21)-(22) are distinct. Controller (24) is used to compute, by means of the optimization process, the required repulsive component of  $\mathbf{f}_{Ei}$ , and thus, because of assumption (ii), of  $\mathbf{f}_{bi}$ . This  $\mathbf{f}_{bi}$  is used in its turn, in (21)-(22), to compute the thruster forces. The controller in (21)-(22) computes a thruster repulsive force twice, once as a PD quantity in (21) and once by means of the  $\mathbf{f}_{ij,r}$  component of  $\mathbf{f}_{bi}$ , in (22). Because of the requirement (b), thrusters in the direction of  $\mathbf{f}_{ij,r}$  are turned off, thus discarding the thruster repulsive force, and allowing only the manipulator to apply the  $\mathbf{f}_{ij,r}$  as an  $\mathbf{f}_{bi}$  component.

In the *point contact* case, (26) is used instead of (23).

$$\mathbf{J}_i^T \mathbf{f}_{Ei} = \begin{bmatrix} \mathbf{f}_{bi}^T & \mathbf{n}_{bi}^T \end{bmatrix}^T \quad (26)$$

Having obtained  $\mathbf{f}_{ij,r}$ , the required end-effector force  $\mathbf{f}_{Ei}$  can also be obtained, as shown earlier in Section IV, and then the servicer actuator inputs are computed using (21), (22) and (23) or (26). In this way, the optimization process (Section IV), which provides the forces  $\mathbf{f}_{Ei}$  acting on the passive object, provides also the forces  $\mathbf{f}_{ij,r}$ , acting on the servicers as components of the reaction of  $\mathbf{f}_{Ei}$  on the servicers. Fig. 3 displays the block diagram of the servicer control process for both contact cases. The differences between the firm grasp case and the point contact case, include a difference in the optimization process ((16) or (19)), a difference at the passive object applied forces/moments ((7) or (8)) and a difference in the calculation of  $\mathbf{n}_{bi}$  ((23) or (26)), see Fig. 3. In both cases, the forces/ moments acting on the passive object are the same.

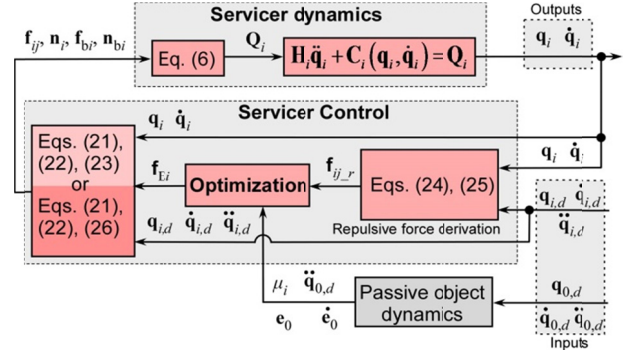


Fig. 3. Flowchart of the servicers control algorithm.

Although servicer bases are subject to switching thrusts, the forces/moments applied by the manipulator on the controlled passive object are continuous. This is because a servicer mass filters thrusts, and because joint motors compensate actively for any residuals, as thruster firing and its effects on the manipulator are known a-priori. Thus the passive object motion can be controlled with vanishing errors, a response that cannot be achieved using only switched forces. The controller stability for the passive object, for both contact-type cases, can be shown using Lyapunov's global stability theorem, with the following Lyapunov function,

$$\dot{V}_0(\mathbf{e}_0, \dot{\mathbf{e}}_0) = \frac{1}{2}(\mathbf{e}_0^T \mathbf{A}_0 \mathbf{K}_{D0}^2 \mathbf{e}_0 + \mathbf{w}_0^T \mathbf{A}_0 \mathbf{w}_0) \geq 0 \quad (27)$$

with  $\mathbf{A}_0 = \text{diag}(a_0(1), \dots, a_0(6)) > 0$  and

$$\mathbf{w}_0 = \dot{\mathbf{e}}_0 + \mathbf{K}_{p0} \mathbf{K}_{D0}^{-1} \mathbf{e}_0 \quad (28)$$

Differentiating (27) and using (1) to (5) for  $i = 0$  along with (14), (7) (or (8)) and (28), we obtain

$$\dot{V}_0 = -\mathbf{e}_0^T \mathbf{A}_0 \mathbf{K}_{D0}^3 \mathbf{e}_0 \leq 0 \quad (29)$$

simply by selecting the following condition

$$\mathbf{K}_{p0} = \mathbf{K}_{D0}^2 \quad (30)$$

Using Barbalat's Lemma [35], it can be shown that

$$\lim_{t \rightarrow \infty} (\dot{V}_0) = 0 \quad (31)$$

and in conjunction to (29), the following is obtained

$$\lim_{t \rightarrow \infty} (\mathbf{e}_0) = 0 \quad (32)$$

Thus, the error  $\mathbf{e}_0$  converges to zero (see (32)), proving the stability of the proposed controller for the passive object. Examining the stability properties of the servicer controllers is more involved. As seen previously, model-based control was used as an intermediate step in developing a switching strategy for the on-off thruster forces. The nature of these forces introduces errors in the relative positions and attitudes between the passive object and each servicer. As mentioned already, these errors need only to remain bounded within certain limits; therefore the lack of asymptotic stability is not a limitation. The boundedness analysis is complicated since some of the forces are continuous (i.e.  $f_{Ei}$ ), while others are switched (i.e.  $f_{ij}$ ). However, the bounded control response can be realized similarly to the on-off attitude control of satellites. The boundedness of servicer motions is demonstrated here via simulation results.

## V. SIMULATIONS RESULTS

To demonstrate the developed methodology, we study the case of three single-manipulator servicers, both when applying *point contact* forces on the passive object and when having a *firm grasp* over it. Each servicer base has thrusters capable of producing forces or moments (thrusters facing the object are deactivated), reaction wheels, and a single PUMA-type manipulator. A series of simulations is run, with realistic parameters in terms of thruster and reaction wheel capabilities. The  $2\text{m} \times 3\text{m} \times 2\text{m}$  orthogonal object has mass of 180 kg. The free-flying servicers have mass of 70 kg each, and their base is of cubic shape with a 0.7 m side. The three contact points lie on the object surfaces with normal vectors parallel to the  $\hat{\mathbf{x}}_0, -\hat{\mathbf{x}}_0$  and  $\hat{\mathbf{y}}_0$  unit vectors of the object body-fixed axes. The servicer thrusters develop per axis a force of 20 N, while their trigger threshold is set to  $f_t = 10$  N. For attitude control, the servicers have additional pairs of thrusters that develop torque of 2 Nm per axis, and reaction wheels that can develop continuous torques up to  $n_t = 1$  Nm per axis. The manipulator on each servicer has a reach of 2.1 m i.e. three times the cubic servicer base side. The above system parameters, including the object/ servicer mass ratio, were chosen taking into account realistic

scenarios. In particular, if the object/ servicer mass ratio is too large, obviously either an extreme number of servicers will be needed, or the task will be physically impossible, depending on the required trajectory. With this ratio too small, the interaction between servicers and the object can be ignored. What is of interest here is the case in which the masses are comparable; this yields the mass of the object. The simulations are run on Matlab/ Simulink. Non-linear constrained optimization function *fmincon* [44] is used to obtain optimal end-effector forces/ torques and contact points. The optimization code running on a current average computer takes about 100 ms. In a dedicated computer with optimized and compiled code, this time will be far smaller, achieving a total loop time close to 100 ms. Although a performance gap between space and ground processors exists, long delays also occur in implementing new methods in space, during which, space-qualified hardware advances; thus this performance should be realizable by future systems.

The motion of all four bodies is simulated with the passive object following a velocity trapezoidal trajectory in all DOF, see Table I. The accelerations were chosen to be compatible with servicer force/ moment capabilities. The desired servicer relative position with respect to the passive object is its initial relative position. This position is chosen so as to accommodate adequately the expected relative motion between each servicer and the passive object, and maintain the manipulator in its kinematic and force workspace [45]. Thus, the servicer position task is to keep the manipulator base at a distance of 1 m for two servicers contacting opposing sides of the passive object and of 0.6 m for the third servicer, measured along the object surface normal vector passing from the end-effector contact point. The servicer attitude control task is to maintain a relative attitude with respect to the object approximately constant.

Table I. Passive object desired motion parameters.

DOF	const. accel. (m/s <sup>2</sup> )/ (rad/s <sup>2</sup> )	up to (s)	const. veloc. (m/s)/ (rad/s)	up to (s)	const. deccl. (m/s <sup>2</sup> )/ (rad/s <sup>2</sup> )	up to (s)
$x_{0\text{des}}$	0.0003	56	0.0168	84	-0.0003	140
$y_{0\text{des}}$	-0.00036	50	-0.018	90	0.00036	140
$z_{0\text{des}}$	0.0002	59	0.0118	81	-0.0002	140
$\theta_{0\text{des}}$	$5 \cdot 10^{-5}$	60	0.003	80	$-5 \cdot 10^{-5}$	140
$\phi_{0\text{des}}$	$7 \cdot 10^{-5}$	55	0.00385	85	$-7 \cdot 10^{-5}$	140
$\psi_{0\text{des}}$	$10^{-4}$	65	0.0065	75	$-10^{-4}$	140

First the case of *point contact* is demonstrated. The bandwidth that corresponds to the control gains is constrained by reaction wheel and thruster limits. Moreover, higher gains would result in lower tracking errors, but more frequent thruster firing, thus higher fuel consumption.

The tradeoff between tracking errors and fuel consumption can be used to obtain the desired gains, for a given desired motion. In this case, the control gains in (14) are  $K_{p0} = 3.24$ ,  $K_{D0} = 1.8$  (for all passive object *translational* DOF),  $K_{p0} = 0.64$ ,  $K_{D0} = 0.8$  (for all passive object

rotational DOF). The gains in (21) and (24) are  $K_{p_i} = K_{r_{p_i}} = 0.16$ ,  $K_{D_i} = K_{r_{D_i}} = 0.4$  (for all servicer *translational* DOF) and  $K_{p_i} = K_{r_{p_i}} = 0.5625$ ,  $K_{D_i} = K_{r_{D_i}} = 0.75$  (for all servicer *rotational* DOF), with  $i = 1, 2, 3$ .

For the desired trajectory in Table I, the actual trajectory is displayed in Fig. 4. Fig. 5 shows the object tracking errors, the servicer base position tracking errors, and the servicer attitude tracking errors, for one of the servicers. For the same servicer, Fig. 6 shows the end-effector applied forces, the servicer thruster forces/ torques, and the reaction wheel torques. The same variables for the other servicers are similar and are not shown here.

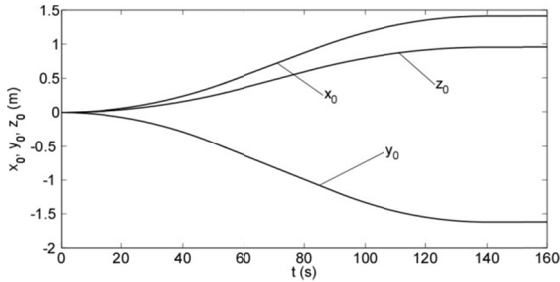


Fig. 4. Actual trajectories of the passive object coordinates.

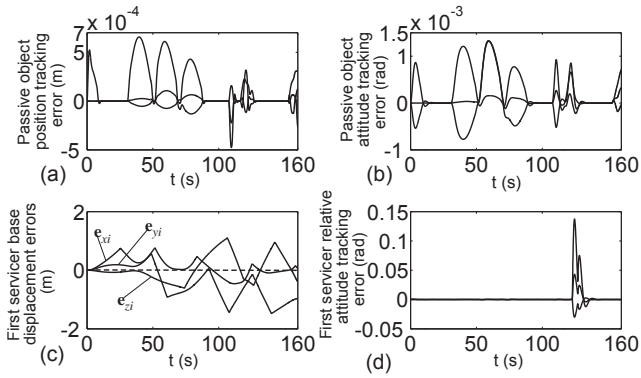


Fig. 5. Point contact case: Tracking errors in (a) object position and (b) attitude, (c) servicer base displacement, and (d) attitude.

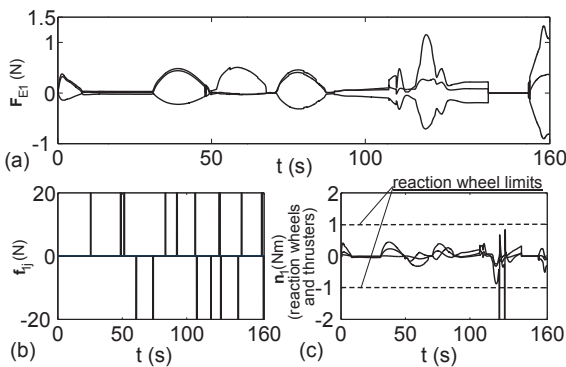


Fig. 6. (a) Typical manipulator applied forces, (b) thruster forces and (c) torques by reaction wheels and thrusters for one of the servicers.

As seen in Figs. 4, 5, and 6, the passive object follows its trajectory very well. The errors in displacements from the desired servicer base location with respect to the object, oscillate around zero, indicating that the manipulator base remains within bounds, see Fig. 5c. Fig. 5d shows very small servicer attitude errors. By increasing the position control

gains of the servicer, the error displacements are reduced accordingly. As expected, more frequent thruster firing is observed, thus increasing the fuel consumption. This behavior demonstrates how the introduction of the manipulators enhances the performance of the system, letting the servicer base move freely in the manipulator workspace, firing the thrusters only when the manipulator approaches its workspace limits, while constantly applying a continuous manipulator force on the passive object. Thus, the servicers filter the infrequent thruster on-off forces, resulting in continuous control forces on the object. As a result, thruster forces are sparse, see Fig. 6b. The moments required by the servicer are low and applied by reaction wheels. If the wheels become saturated, torque-thrusters fire-up, operating at one-tenth of the thruster maximum propulsion capability, see Fig. 6c.

In Fig. 7a, the manipulator joint angles for the first servicer, as well as their physical limits, are shown, for the case of a PUMA-like manipulator, see Fig. 2 (with angles  $\theta_{11}$  and  $\theta_{12}$  corresponding to the joints at the base of the manipulator and with axes parallel to the servicer base  $z$  and  $y$  axes respectively). In Fig. 7b, the corresponding joint torques are shown. As can be seen, no angle exceeds manipulator reasonable physical limits, while the torque requirements are quite acceptable. Note that the physical limits for both angles  $\theta_{11}$  and  $\theta_{12}$  are  $\pm 90$  deg. The sudden changes in the slope of the joint angles responses are due to thruster firing or to manipulator pushing the servicer away from the passive object (in both cases, there is a change in servicer direction).

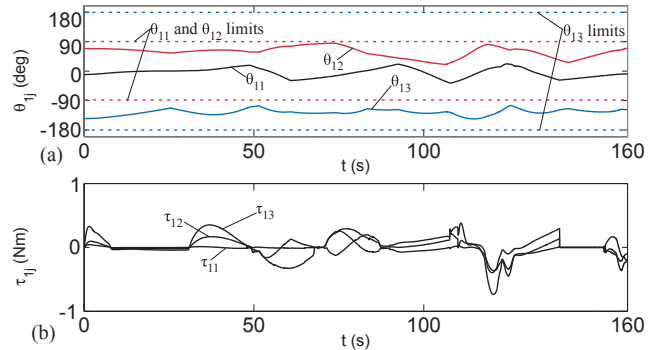


Fig. 7. Typical manipulator joint-angles (a) and joint-torques (b).

As shown in Fig. 7a, the typical manipulator joint-angles vary around their initial values, keeping the manipulator end-effectors well into their workspace. These variations can be reduced further by increasing control gains  $K_{p_i}$ ,  $K_{r_{p_i}}$ ,  $K_{D_i}$  and  $K_{r_{D_i}}$ . Then, smaller servicer base deviations around their desired (initial) positions and smaller variations of the corresponding manipulator joint-angles  $\theta_{ij}$  from their initial values will result. Higher gains are expected to lead to more frequent thruster firing and therefore increased consumption of fuel. This tradeoff can be resolved by system operators.

To show this, we assume that fuel consumption is proportional to the integral of all thruster forces, and compare the response corresponding to the initial gains with that that results from a set of higher gains,  $K_{p_i} = K_{r_{p_i}} = 0.25$ ,  $K_{D_i} = K_{r_{D_i}} = 0.5$ . A direct comparison between Fig. 8a to

Fig. 8b shows that manipulator joint angles vary less around their initial positions for higher gains, while a comparison between Fig. 8c and Fig. 8d shows that fuel consumption has increased by more than 25%.

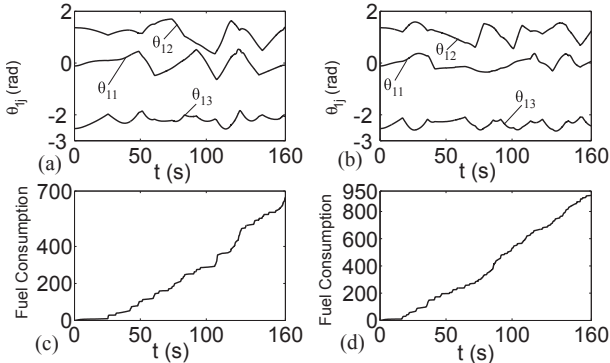


Fig. 8. Typical manipulator joint-angles and fuel consumption, for the initial servicer control gains (a and c) and for increased gains (b and d).

The response of the developed control law is compared to the one where the forces/torques are applied to the passive object by thruster equipped servicers (without manipulators) in direct contact to it and actuated by (a) pure on-off control with a deadband and, (b) by PWPF control, for the same passive object desired motion (Table I). All mass properties and the desired trajectory are kept the same. In both cases, the control law is model-based as in (14), where the required  $Q_0$  is transformed to the passive object frame.

In the pure on-off control case, each thruster is turned on, when the corresponding continuous force or torque value exceeds a preset threshold value  $f_i$  or  $n_i$  respectively. The control gains were chosen as  $K_{p0} = 2.25$ ,  $K_{D0} = 1.5$  (for all passive object *translational* DOF),  $K_{p0} = 6$ ,  $K_{D0} = 3$  (for all passive object *rotational* DOF), while the threshold values were chosen as  $f_i = 18\text{N}$  and  $n_i = 1\text{Nm}$ . In the PWPF case, the PWPF modulator developed in [45] was employed. The control gains and the signal filter parameters were chosen as  $K_{p0} = 12.25$ ,  $K_{D0} = 3.5$ ,  $K_m = 1$ ,  $\tau_m = 0.5$  (for all passive object *translational* DOF),  $K_{p0} = 9$ ,  $K_{D0} = 3$ ,  $K_m = 1$ ,  $\tau_m = 0.95$  (for all passive object *rotational* DOF), while the threshold  $U_{on} = [f_i^T n_i^T]^T$  values were chosen as  $f_i = 18\text{N}$  and  $n_i = 1\text{Nm}$  and the  $U_{off}$  values (hysteresis) were set at 80% of the  $U_{on}$  ones (thus leading to  $h_{trans} = 3.6$  and  $h_{rot} = 0.20$ ). These parameters ensure minimum pulse duration of 100 ms. The applied thruster forces/ torques were again 20N and 2Nm respectively, for both the pure on-off and PWPF cases.

Fig. 9 shows the tracking errors and the corresponding fuel consumption as a function of time, obtained again as in Figs. 8c and 8d. In this figure, it can be seen that the performance of the proposed system is superior to that of the system without manipulators, for both PWPF and pure on-off control cases. Indeed, for the same fuel consumption (Figs. 9a and 9b), the position error for the proposed system is approximately *six* times less than the one for the PWPF control (Figs. 9d and 9e). Moreover, it can be seen that the performance of the PWPF control system is, as expected, superior to that of the pure on-off control, since, for slightly higher maximum tracking errors for the pure on-off control case (Figs. 9e and 9f) the fuel consumption is more than

double (Fig. 9b and 9c). The tracking error of both the PWPF and the pure on-off control can be lowered with higher control gains (or equally with lower triggering thresholds), but that would result in a further increase in the fuel consumption. Moreover, the fuel consumption of the pure on-off control system can be lowered to the levels of the other two systems, but that would result in very high tracking errors. Note that for the thrusting of servicer bases with manipulators, pure on-off control was used for simplicity. If PWPF control were used, the fuel consumption of the proposed system would be even lower.

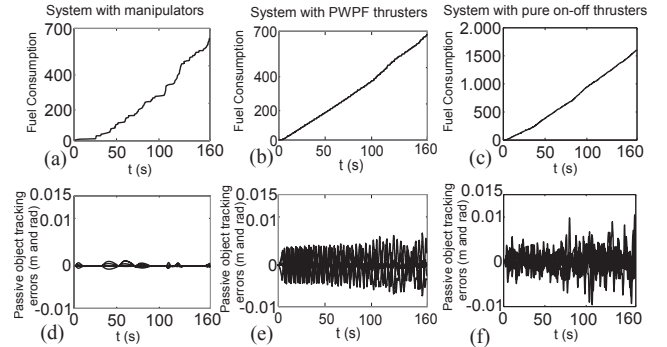


Fig. 9. Tracking error and corresponding fuel consumption as a function of time. (a), (d) with manipulators, (b), (f) without manipulators (PWPF thrusters), and (c), (e) without manipulators (pure on-off thrusters).

To investigate controller robustness to parameter variations, parametric inaccuracies, lag in applying thruster forces, and error in the application of a manipulator force were introduced, see Table II. The same controller and gains as before were used. Fig. 10 displays the same variables as those of Fig. 5. It can be seen that the tracking capability of the system is still remarkable, while the servicers are again within their workspace limits.

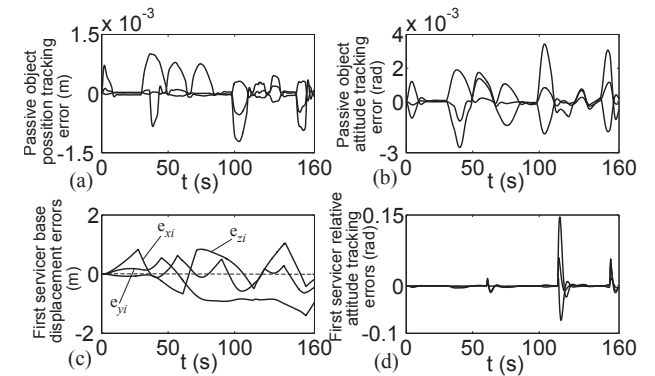


Fig. 10. Point contact case with inaccuracies: Tracking errors in (a) object position and (b) attitude, (c) servicer base displacement, and (d) attitude.

Several more simulations with various inaccuracies were run and had similar results; they are not shown here for brevity. These show that the developed controller is reasonably robust with respect to parametric and modeling errors. The developed controller can be extended to include adaptive capabilities. However, one should first consider the benefit in the resulting response versus the complexity and limitations of such algorithms.

Table II. Introduced Inaccuracies

Object mass error	Object center of mass position error	Thruster $f_{34}$ lag	Thruster $f_{23}$ lag	Error in force $f_{E1}$
-20%	-10%	0.4 s	0.4 s	-10%

The same desired motion scenario is simulated for the case of *firm grasp*. In Fig. 11, the same variables as in Fig. 5 are shown for the case of firm grasping. In Fig. 12, a comparison on tracking errors and fuel consumption is being made, between the case of point contact (Fig. 12 a, c) and firm grasp (Fig. 12 b, d). It can be seen that, as expected, the case of firm grasping of the passive object by the servicer manipulators, displays even lower fuel consumption, with far lower tracking errors on the motion of the passive object.

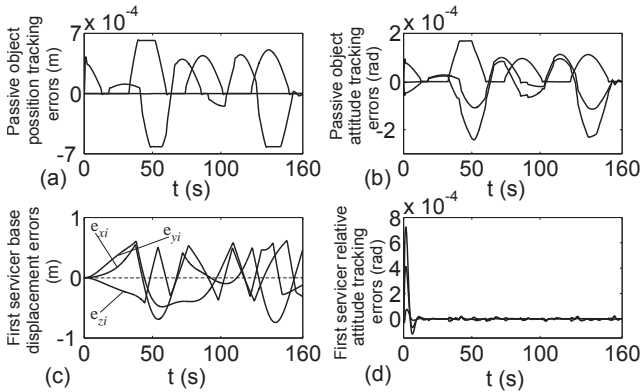


Fig. 11. (a) Firm grasp case: Tracking errors in (a) object position and (b) attitude, (c) servicer base displacement, and (d) attitude.

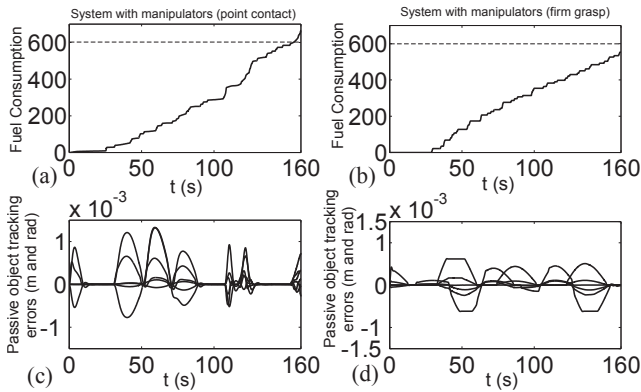


Fig. 12. Tracking error history and corresponding consumed fuel for servicers with manipulators. (a), (c) firm grasp case, (b), (d) point contact.

## VI. CONCLUSIONS

This work has studied the handling of an on orbit passive object via servicers, employing both on-off thrusters and manipulator continuous forces. In this technique, the on-off forces are filtered by the manipulator-servicer system, allowing accurate passive object motion and reducing fuel consumption. The dynamics of three cooperating single-manipulator free-flying robotic servicers, handling a larger passive rigid object for the cases of firm grasps and for point contacts were studied. Using a two-layer optimization process, a planning strategy for trajectory tracking of a passive object including optimal end-effector contact point

selection and an adapted model-based controller, were developed. For both cases studied, the performance of the manipulation method was shown by simulations to exhibit desirable response characteristics, such as remarkable positioning accuracy and reduced thruster fuel consumption.

## REFERENCES

- [1] Tatsch, A., Fitz-Coy, N. and Gladun, S. "On-orbit Servicing: A Brief Survey," Performance Metrics for Intelligent Systems Conf., Gaithersburg, MD, August 15 - 19, 2006.
- [2] Rekleitis, I., Martin, E., Rouleau, G., L'Archevêque, R., Parsa, K., and Dupuis, E., "Autonomous Capture of a Tumbling Satellite", J. of Field Robotics, Special Issue on Space Robotics, 2007, 24(4), pp. 275-296.
- [3] Kaiser, C., Rank, P., Krenn, R., "Simulation of the Docking Phase for the SMART-OLEV Satellite Servicing Mission," i-SAIRAS: Int. Symposium on Artificial Intelligence, Robotics and Automation in Space, Hollywood, USA, February 26-29, 2008.
- [4] Yoshida, K., "ETS-VII Flight Experiments For Space Robot Dynamics And Control," Int. Symposium on Experimental Robotics, Waikiki, Hawaii, USA, December 10-13, 2000.
- [5] <http://www.darpa.mil/orbitalexpress/>
- [6] Khatib, O., "Mobile manipulation: The robotic assistant," Robotics and Autonomous Systems, 1999, 26(2-3), pp. 175-183.
- [7] Chang, K.-S., Holmberg R. and Khatib, O., "The Augmented Object Model: Cooperative Manipulation and Parallel Mechanism Dynamics," IEEE Int. Conf. on Robotics & Automation (ICRA '00), San Francisco, CA, USA, April 24-28, 2000.
- [8] Li, Q., Payandeh, S., "Planning for dynamic multiagent planar manipulation with uncertainty: a game theoretic approach," Systems, Man & Cybernetics, Part A: Systems & Humans, 2003, 33(5), pp. 620-626.
- [9] Tang, C. P., Bhatt, R. M., Abou-Samah, M., and Krovi, V., "Screw-Theoretic Analysis Framework for Payload Transport by Mobile Manipulator Collectives," IEEE/ASME Transactions on Mechatronics, 2006, 11(2), pp. 169-178.
- [10] Caccavale, F., Chiacchio, P., Chiaverini, S., "Task-space regulation of cooperative manipulators", Automatica, 2000, 36, pp. 879-887.
- [11] Fink, J., Hsieh, M. A., Kumar, V., "Multi-Robot Manipulation via Caging in Environments with Obstacles," IEEE Int. Conf. on Robotics and Automation (ICRA '08), Pasadena, CA, USA, May 19-23, 2008.
- [12] Esposito, J., Feemster M., and Smith, E., "Cooperative Manipulation on the Water Using a Swarm of Autonomous Tugboats," IEEE International Conference on Robotics and Automation (ICRA '08), Pasadena, CA, USA, May 19-23, 2008.
- [13] Miyata, N., Ota, J., Arai, T., Asama, H., "Cooperative transport by multiple mobile robots in unknown static environments associated with real-time task assignment," IEEE Transactions on Robotics and Automation, 2002, 18(5), pp. 769-780.
- [14] Rus, D., Donald, B., Jennings, J., "Moving furniture with teams of autonomous robots," IEEE/RSJ Int. Conf. on Intelligent Robots and Systems (IROS '95), Pittsburgh, USA, August 5-9, 1995.
- [15] Fernández, F., Parker, L., "Learning in large cooperative multi-robot domains," Int. J. of Robotics and Automation, 2001, 16(4), 217-226.
- [16] Kao, I., Lynch, K., Burdick, J., Handbook of Robotics, Chapter 27: Contact Modeling and Manipulation, Springer, 2008.
- [17] Moosavian, A., Papadopoulos, E., "Cooperative Object Manipulation with Contact Impact Using Multiple Impedance Control," International Journal of Control, Automation, and Systems (IJCAS), 2010, Vol. 8, No. 2, pp. 314-327.
- [18] Matsumoto, S., Wakabayashi, Y., Ueno, H., Nishimaki, T., "System Analyses and Feasibility Studies for Hyper-OSV (Orbital Servicing Vehicle)," i-SAIRAS: Int. Symp. on Art. Intell., Robotics & Automation in Space, CSA, St-Hubert Que., Canada, June 18-22, 2001.
- [19] Yoshida, K., Nakanishi, H., "The TAKO (Target Collaborativize) Flyer: A New Concept for Future Satellite Servicing," i-SAIRAS: Int. Symposium on Artificial Intelligence, Robotics and Automation in Space, CSA, Quebec, Canada, June 18-22, 2001.
- [20] Dubowsky, S., Boning, P., "The Coordinated Control of Space Robot Teams for the On-Orbit Construction of Large Flexible Space Structures," Int. Conf. on Robotics and Automation (ICRA '07), Special Workshop on Space Robotics, Rome, Italy, April 10-14, 2007.

- [21] Hiramatsu, T., Fitz-Coy, N., "Game Theoretic Approach to Post-Docked Satellite Control," 20th Int. Symposium on Space Flight Dynamics, Goddard Space Flight Center, USA, September 24, 2007.
- [22] Moosavian, S. A. A., Rastegarij R., and Papadopoulos, E., "Multiple Impedance Control for Space Free-Flying Robots," AIAA Journal of Guidance, Control and Dynamics, 2005, Vol. 28, No. 5, pp. 939-947.
- [23] Toglia, C., Kennedy, F., Dubowsky, S., "Cooperative Control of Modular Space Robots," Autonomous Robots, in Press, DOI: 10.1007/s10514-011-9238-z.
- [24] Everist, J., Mogharei, K., Suri, H., Ranasinghe, N., Khostnevis, B., Will, P. and Shen, W., "A System for In-Space Assembly," 2004 IEEE/RSJ Int. Conf. on Intelligent Robots and Systems (IROS '04), Sendai, Japan, September 28 - October 02, 2004.
- [25] Rekleitis G. and Papadopoulos, E., "Towards Passive Object On-Orbit Manipulation by Cooperating Free-Flying Robots," Proc. IEEE International Conference on Robotics and Automation (ICRA '10), Anchorage, Alaska, USA, May 03-08, 2010.
- [26] Rekleitis G. and Papadopoulos, E., "On On-Orbit Passive Object Handling by Cooperating Space Robotic Servicers," Proc. IEEE/RSJ International Conference on Intelligent Robots and Systems (IROS '11), San Francisco, California, USA, September 25-30, 2011.
- [27] Bryson, A. E., Control of Spacecraft and Aircraft, Princeton University Press, 1994.
- [28] Kienitz, K., "Attitude stabilization with actuators subject to switching restrictions: an approach via exact relay control methods," IEEE Tr. Aerospace and Electronic Systems, 2006, 42(4), pp. 1485-1492.
- [29] ASTRIUM, "1 N Mono-Propellant Thruster," Datasheet, 2012 <http://cs.astrium.eads.net/sp/brochures/thrusters/1N%20Thruster.pdf>
- [30] Anthony, T. C., Wie, B., Carroll, S., "Pulse-Modulated Control Synthesis for a Flexible Spacecraft," Journal of Guidance, Control, and Dynamics, Vol. 13, No.6, pp.1014-1021, 1990.
- [31] Song, G., Buck, N. V., Agrawal, B. N., "Spacecraft Vibration Reduction Using Pulse-Width Pulse- frequency Modulated Input Shaper," Journal of Guidance, Control, and Dynamics, 22 (3), pp. 433-440, 1999.
- [32] Singh, T., Heppler, G. R., "Shaped Input Control of a System with Multiple Modes," Journal of Dynamics System, Measurement, and Control, Vol. 115, pp. 341-344, 1993
- [33] Arantes Jr., G., Martins-Filho, L. S., Santana, A. C., "Optimal On-Off Attitude Control for the Brazilian Multimission Platform Satellite," Mathematical Problems in Engineering, Hindawi, Volume 2009, Article ID 750945, doi:10.1155/2009/750945.
- [34] Moosavian, S. A. A., Papadopoulos, E., "Explicit Dynamics of Space Free-Flyers with Multiple Manipulators via SPACEMAPLE," Advanced Robotics, Robotics Society of Japan, Vol. 18, No. 2, pp. 223-244, 2004.
- [35] Krstic, M., Kanellakopoulos, I., Kokotovic, P., Nonlinear and Adaptive Control Design. Wiley-Interscience, 1995.
- [36] An, C. H., Atkeson, C. G., Hollerbach, J. M., Model-based control of a robot manipulator, MIT Press, 1988.
- [37] Gautier, M., Khalil, W., Restrepo, P. P., "Identification of the dynamic parameters of a closed loop robot," Proc. IEEE International Conference on Robotics and Automation (ICRA '95), Nagoya, Aichi, Japan, April 09-11, 1995.
- [38] Furukawa, T., Sugata, T., Yoshimura, S., Hoffman, M., "An automated system for simulation and parameter identification of inelastic constitutive models," Computer Methods in Applied Mechanics and Engineering, 2002, 191(21-22), pp. 2235-2260.
- [39] Kumar, V., Waldron, K. J., "Suboptimal algorithms for force distribution in multifingered grippers," IEEE Transactions on Robotics and Automation, 1989, 5(4), pp 491-498.
- [40] Chen, F.-T., Orin, D. E., "Optimal force distribution in multiple-chain robotic systems," IEEE Transactions on Systems, Man and Cybernetics, 1991, 21(1), pp 13-24.
- [41] Bicchi, A., "Force distribution in multiple whole-limb manipulation," Proc. IEEE International Conference on Robotics and Automation (ICRA '93), Atlanta, Georgia, USA, May 02-06, 1993.
- [42] Chen, Y.-C., Walker, I. D., Cheatham, J. B., "A new approach to force distribution and planning for multifingered grasps of solid objects," Proc. IEEE International Conference on Robotics and Automation (ICRA '91), Sacramento, CA, USA, April 09-11, 1991.
- [43] Cornella, J., Suarez, R., Carloni, R., Melchiori, C., "Dual programming based approach for optimal grasping force distribution," Mechatronics, 2008, 18(7), pp. 348-356.
- [44] <http://www.mathworks.com/help/optim/ug/fmincon.html>
- [45] Papadopoulos, E. and Gonthier, Y., "A Framework for Large-Force Task Planning of Mobile Redundant Manipulators," Journal of Robotic Systems, Vol. 16, No 3, 1999, pp. 151-162.
- [46] Arantes Jr., G., Martins-Filho, L. S., Santana, A. C., "Optimal On-Off Attitude Control for the Brazilian Multimission Platform Satellite," Mathematical Problems in Engineering, Volume 2009, Article ID 750945, 17 pages, doi:10.1155/2009/750945, Hindawi Publishing Corporation, 2009.



**Georgios Rekleitis** (S'11) received his Diploma from the University of Patras, in 2001 and his MEng degree from the Mechanical Engineering Department at McGill University in 2003. His current research interests are in the area of space robotics, cooperative manipulation, control and modeling of dynamic systems.

He is a member of the Technical Chamber of Greece (TEE) and Student

Member of IEEE and AIAA.



**Evangelos Papadopoulos** (S'83–M'91–SM'97) received his Diploma from the National Technical University of Athens (NTUA) in 1981, and his M.S. and Ph.D. degrees from MIT in 1983 and 1991 respectively, all in Mechanical Engineering. He was an analyst with the Hellenic Navy, Athens, Greece, from 1985 to 1987. In 1991 he joined McGill U. and the Centre for Intelligent Machines (CIM) as an Assistant Professor. Currently, he is a Professor with the Department of Mechanical Engineering at the NTUA.

He teaches courses in the areas of Systems, Controls, Mechatronics and Robotics. His research interests are in the area of robotics, modeling and control of dynamic systems, mechatronics and design. He serves as an Associate Editor for the *ASME J. of Dynamic Systems, Measurement and Control*, and the *Machine and Mechanism Theory*, while previously he served as an Associate Editor of the *IEEE Transactions on Robotics*, and as a Guest Editor for the *IEEE/ASME Transactions on Mechatronics*. He has published more than 200 technical articles in journals and refereed conference proceedings. He is a Senior Member of AIAA and a Member of the ASME, the Technical Chamber of Greece and Sigma Xi.